Transient Analysis of a Two-Phase Flow Natural Circulation Loop using a Separated Two-Phase Flow Model

***Paul T Senda*[a] *and Robert T Dobson*[b]**

[a] *Cape Peninsula University of Technology, Cape Town, South Africa, ptsenda@gmail.com*
[b] *Stellenbosch University, Stellenbosch, South Africa, rtd@sun.ac.za*

Abstract:

In this paper the transient and dynamic behaviour of a natural circulation heat transfer loop of 32 mm inside diameter, 7 m height and 8 m width, using water as working fluid is theoretically simulated and experimentally validated. The theoretically simulation requires that the loop is discretised into a number of cylindrical symmetrical control volume and the conservation of mass, momentum and energy are applied to the control volume. The separated two-phase flow model uses frictional multiplier and vapour-liquid void fraction correlations similar to those originally suggested by Martinelli. An orifice plate is used to measure the mass flow rate and which is then compared with the calculated mass flow rate. It is concluded that the theoretical model using the separated two-phase model adequately captures the actual transient and dynamic flow and heat transfer behaviour of the loop. It is further concluded that for future studies of natural two-phase circulation systems the mathematical model using the separated two-phase flow as presented theoretical simulation may be confidently used.

Keywords:

Heat transfer loop, Natural circulation, Separated two-phase flow model, Transient behaviour, Control volume.

1. Introduction

In this paper the transient behaviour of a natural circulation loop will be theoretically simulate using the separated two-phase model and experimentally validated using a 7 m height and 8 m width natural circulation loop shown in Figure 1.

A natural circulation loop is also called a loop thermosyphon. It is a thermo-fluid design that works with temperature induced density gradients to create the natural circulation of the working fluid in the system. A loop thermosyphon operates as the natural convection of the liquid when heat added to the liquid; it gives rise to a temperature difference from one side of the loop to the other where the warmer fluid is less dense and thus more buoyant than the cooler fluid on the other side of the loop [1]. With the assistance of gravity, the liquid will move from the denser section (condenser section) to the less dense section (evaporator section). Here the liquid will be heated and pushed again toward the condenser. The process is also self-controlling as the temperature difference increases, so too do the heat transfer rate and flow rate ([2], [3]).

Thermosyphon loops have many applications and can be used in many technologies [3] such as solar, ventilation, nuclear etc. In the nuclear industry they are used as passive systems, hence also inherently safe, making them particularly suitable for use in this industry; where reliability and safety are vital. For instance, they may be used in high temperature reactors in the reactor cavity cooling system (RCCS) .

2. Natural circulation loop experimental setup

This section describes the experimental setup of the natural circulation loop used to collect data in order to validate the theoretical simulation. This section also looks at the loop with particular focus to its geometry and characteristics and instruments used to capture and acquire data. The process followed during experimentation is also provided.

2.1 Experimental setup

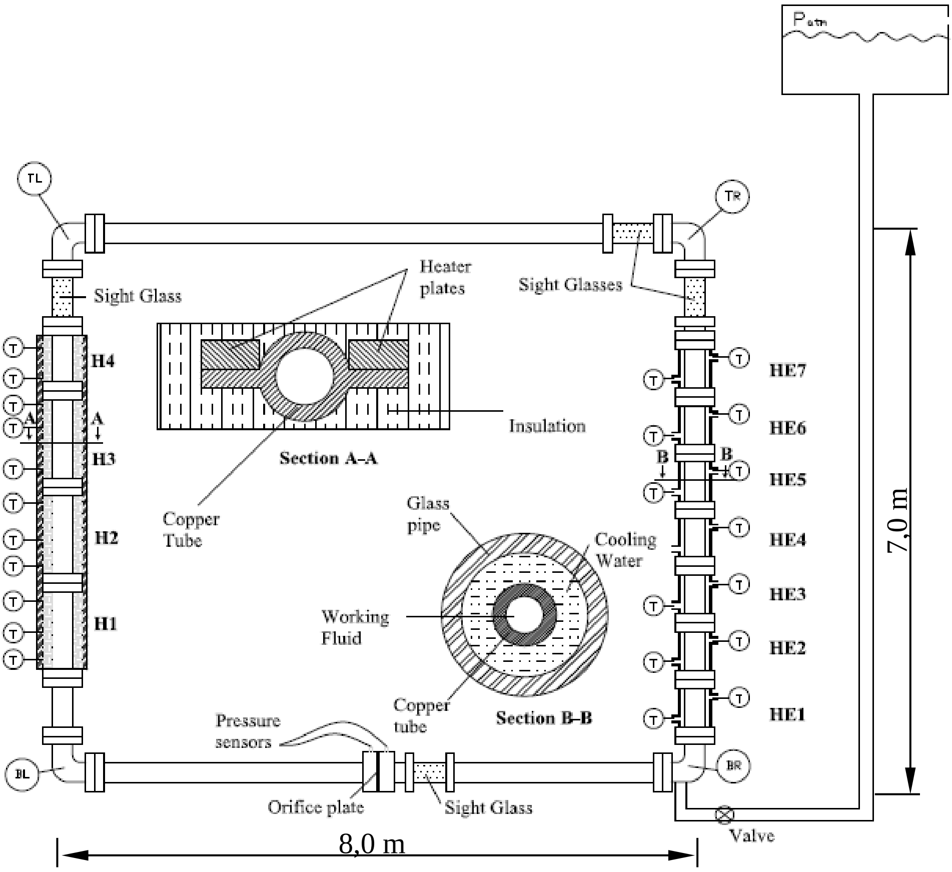

Fig. 1. Schematic representation of the Experimental thermosyphon loop setup

Figure 1 shows the 7 m height and 8 m wide diagrammatic representation of the rectangular experimental setup. The loop was designed and constructed by Sittmann [4] using copper tubes of 32 mm inside diameter and 3 mm wall thickness. Copper is used due to its high thermal conductivity thereby making its thermal resistance very small compared with the inside and outside heat transfer coefficient and can therefore be neglected. Four transparent polycarbonate sight glasses are incorporated in the loop positioned as shown in Figure 1 for viewing the working fluid flow in the loop. Water is used as the working fluid for the experimental tests due of its cost, availability, abundance and the knowledge and easy use of its heat transfer properties.

The loop has two vertical legs; the heated leg or evaporator section at the LHS where heat is input into the system and the cooled leg or condenser section at the RHS of the loop and where heat is removed. The evaporator section consists of four heating plate elements designated by H1, H2, H3 and H4 from the bottom respectively. Three heating plate (H1, H2 and H3) are of same dimensions (i.e. 1.85 m length, 50 mm wide and 10 mm thick) and have a resistance of 35 Ω each capable of producing 1500 W of heat, and the fourth (H4) on top is identical to the first three, however it is only 650 mm in length with a resistance of 105 Ω capable of providing 500 W of heat.

The condenser section consists of seven pipe-in-pipe heat exchangers (HE1, HE2, HE3, HE4, HE5, HE6 and HE7) arranged from the bottom to the top respectively. Six HEs consist of a 1 m copper pipe onto which two glass outer pipes are attached using a custom made copper alloy connector and silicon O-rings yielding a total cooled length of 1.85 m and HE (in the top) consists of a 650 mm copper pipe and a 550 mm glass outer pipe.

2.2 Sensors and data acquisition

An orifice plate is used to capture the oscillatory flow-behaviour during the experiments. A calibrated differential pressure transducer (Celebar S Endress & Hauser (E&H) IP66/IP67 PMD75 model pressure transducer No S/N A806930109D with sensor range of -500 to 500 mbar and a maximum permissible error of ±0.1%) is used to record and measure the mass flow rate. This pressure transducer was calibrated using a van Essen BETZ type 5000 having a measuring range of -10 to 5000 Pa (gauge pressure) and an accuracy of ± 0.2 Pa.

Twenty three K-type thermocouples are calibrated and used to measure the temperatures of the working fluid, heating plates and cooling water. They are connected to a 34970A Agilent data acquisition, serial number MY44045582 carrying two cards of 20 channels each. Both cards are used and each thermocouple is kept in a specific channel for the duration of the experiments. The data logger is set to collect data points every 10 ms intervals, but only records an averaged value every 1.445 s.

2.3 Experimental procedure

The loop was filled with water from the bottom via the pipe connecting the expansion tank to the loop and letting; at the same time air escapes from the purge valve, located at the highest point in the loop. When no more air and only water escapes the purge valve is closed. The system is then heated and the air in solution is released it collects at the highest point of the loop where it can be periodically purged. The working fluid is allowed to cool down and the above process is repeated a number of times until no more air collect at purge valve. This is important as if the air is not removed it may collect as an insulting layer in the condenser section and thereby decreasing the heat transfer rate in the condenser.

The power may then be switched on; normally the power is increased in steps from 30%, 50%, 70% to 100% of the full power of 9.4 kW, and the data measured and logged. As the power is increased the water will eventually boil and it will be pushed back into the expansion tank. During this process care must be taken, by changing the power input level, to insure steady operation without all the water being pushed in the expansion tank by carefully controlling the condenser cooling water flow rate.

3. Mathematical modelling

In order to theoretically simulate the loop thermosyphon, the loop is discretised into a number of cylindrical shaped control volumes as depicted in figure 2, the simplifying assumptions made before applying the conservation equations to each control volume and use the separated two phase flow to compute the transient behaviour of the working fluid.

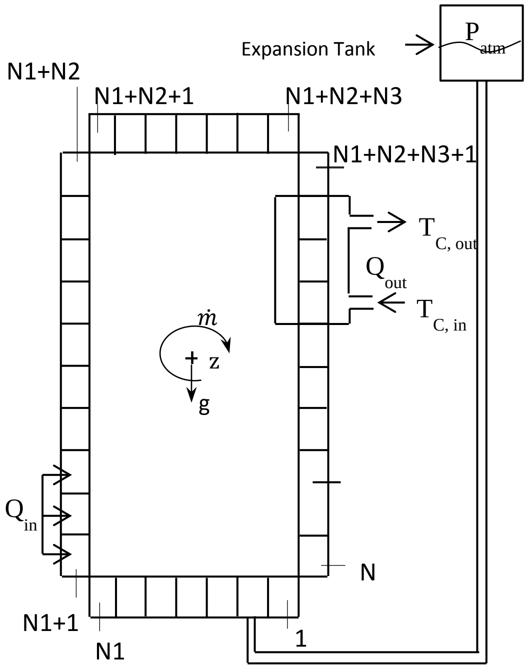

Fig. 2. Discretisation schematic of the natural circulation theoretical

3.1 Simplifying assumptions

Several assumptions are made to simplify the mathematical model of the discretised loop as shown in Figure 2. The assumptions imply that control volumes are one-dimensional at any cross-section area along the axis of the flow [5]. At any instant in time the mass flow rate is in a quasi-equilibrium condition ([6], [7]). At any cross-section both the liquid and gas streams are in thermodynamic equilibrium with each other [8].

3.2 Conservation equations

The conservation of mass, momentum and energy are applied to each control volume as shown in Figure 3, in order to develop differential equations needed for the theoretical simulation.

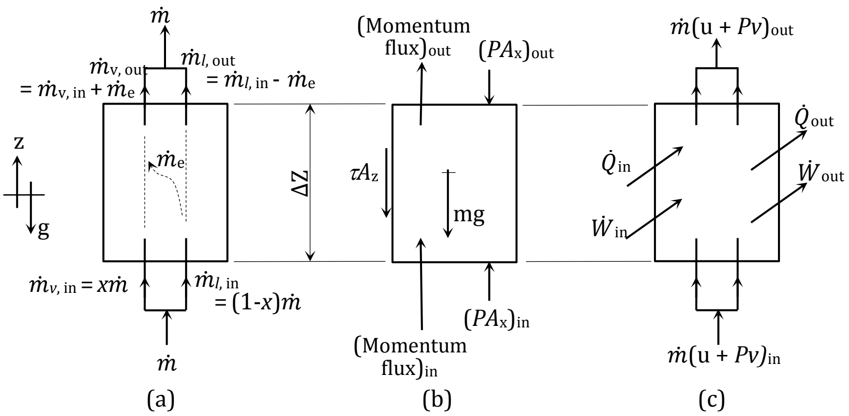

Fig. 3. Conservation of (a) mass, (b) momentum and (c) energy as applied to a representative control volume

The conservation of mass is applied as in (1) to the control volume as shown in Figure 3(a) in order to determine the amount of mass transferred from the expansion tank.

$$\frac{\Delta m}{\Delta t} = \dot{m}_{in} - \dot{m}_{out} \qquad \text{[kg/s]} \tag{1}$$

Equation (1) can also be represented in an explicit form as shown in (2)

$$m_i^{t+\Delta t} = m_i^t + \Delta \mathrm{t}(\dot{m}_{in} - \dot{m}_{out})_i^t \tag{2}$$

where $m = \rho A_x \Delta z$ and $\dot{m} = \rho v A_x = \rho G$ since $v = G/A_x$ and $A_x = \pi d^2/4$, ρ is the density of the working fluid, G is the volumetric flow rate and d is the pipe diameter of the loop.

For the control volume (i) the density given in (3) is determined knowing the mass m_i, the mass flow rate $\dot{m}_i$ and the volume V_i of the control volume.

$$\rho_i^{t+\Delta t} = m_i^{t+\Delta t}/V_i \tag{3}$$

Equation (1) introduces the new mixture mass, therefore the new phase masses will be given function of the mass fraction x, and the new volume function of the void fraction α [9] as $m_v = xm$, $m_l = (1-x)m$, $V_v = \alpha V$ and $V_l = (1-\alpha)V$.

Applying the conservation of momentum to the control volume as shown in Figure 3(b), (4) is found

$$\frac{\Delta}{\Delta t}(mv) = (\dot{m}v)_{in} - (\dot{m}v)_{out} + (PA)_{in} - (PA)_{out} - m_i g \sin\theta - \tau A_z \tag{4}$$

where v is the velocity of the fluid, P is the pressure on the control volume and A is the area.

For a single phase flow model; or using $v = \dot{m}/\rho A$ and dividing throughout by the cross sectional area A, as shown in (5).

$$\frac{\Delta}{\Delta t}\left(\frac{m\dot{m}}{A\rho}\right) = \left(\frac{\dot{m}^2}{A\rho}\right)_{in,i} - (\dot{m}v)_{out,i} + (PA)_{in,i} - (PA)_{out,i} - m_i g \sin\theta_i - \tau A_z \tag{5}$$

For a separated two-phase flow model, after dividing throughout by the cross sectional area A of the control volume and making use identities, the momentum equation may be expressed in terms of the mass, mass flow rate, void fraction and mass fraction as in (6)

$$\begin{aligned}\frac{\Delta}{\Delta t}\left[\frac{m\dot{m}}{A^2}\left(\frac{x^2}{\alpha\rho_v} + \frac{(1-x)^2}{(1-\alpha)\rho_l}\right)\right]_i &= \frac{\dot{m}^2}{A_i}\left[\left(\frac{x^2}{\alpha A\rho_v} + \frac{(1-x)^2}{(1-\alpha)A\rho_l}\right)_{in} - \left(\frac{x^2}{\alpha A\rho_v} + \frac{(1-x)^2}{(1-\alpha)A\rho_l}\right)_{out}\right] \\ &+ P_{in,i} - P_{out,i} - [(\alpha\rho_v + (1-\alpha)\rho_l) g \sin\theta\,\Delta z]_i - \left[\frac{\tau_{lo}\phi_{lo}^2 A_z}{A}\right]_i \end{aligned} \tag{6}$$

where $m = (\alpha\rho_v + (1-\alpha)\rho_l)A\Delta z$ in the new mass.

In accordance with the concept of upwind differencing for the momentum flux term (the first term on the right hand side of (6)) $in = i - 1$ if $\dot{m} \geq 0$ and $in = i + 1$ if $\dot{m} < 0$ and "out" always equals "in", irrespective of the flow direction.

The conservation of energy was applied in terms of the *thermal energy u* equation to the control volume in Figure 3.2(c) to generate (7).

$$\frac{\Delta}{\Delta t}(mu) = (\dot{m}u)_{in} - (\dot{m}u)_{out} + \dot{Q}_{in} - \dot{Q}_{out} + (PAv)_{in} - (PAv)_{out} - \tau_w A_z v \ \text{[W]} \tag{7}$$

where τ is the shear stress.

Equation (7) can be written explicitly as (8)

$$u_i^{t+\Delta t} = \left[(mu)_i^t + \Delta t \sum \dot{E}_i^t\right]/m_i^{t+\Delta t} \tag{8}$$

where some of energy rate is given in (9).

$$\sum \dot{E}_i^t = \left[(\dot{m}u)_{in} - (\dot{m}u)_{out} + \dot{Q}_{in} - \dot{Q}_{out} + (PAv)_{in} - (PAv)_{out} - \tau_w A_z v\right]_i^t \tag{9}$$

All thermodynamic properties will then be a represented function of internal energy $u_i^{t+\Delta t}$ and the density $\rho_i^{t+\Delta t}$; $f(u_i^{t+\Delta t}, \rho_i^{t+\Delta t})$.

3.3 Separated two-phase flow

The separated two-phase flow model is used to represent the properties and behaviour of the control volumes containing both liquid and steam streams [10].

Applying the conservation of mass on the control volume of such two-phase model, (2) becomes (10) in terms of mass or (11) in terms of the mass flow rate

$$m = m_v + m_l = xm + (1-x)m \quad (10)$$

$$\dot{m} = \dot{m}_v + \dot{m}_l, \dot{m}_v = \rho_v \dot{m}_v A_v \text{ and } \dot{m}_l = \rho_l \dot{m}_l A_l \quad (11)$$

Where x is the mass fraction defined by (12) and ρ defined as shown in (13)

$$x = \frac{m_v}{m_v+m_l} = \frac{\dot{m}_v}{\dot{m}_v+\dot{m}_l} \quad (12)$$

$$\rho = \alpha\rho_v + (1-\alpha)\rho_l \quad (13)$$

where the *void fraction* α is defined by (14)

$$\alpha = \frac{V_v}{V_v+V_l} = \frac{\dot{V}_v}{\dot{V}_v+\dot{V}_l} = \frac{A_v}{A_v+A_l} \quad (14)$$

The void fraction may also be expressed as in (15)

$$\alpha = \left(1 + \frac{v_v}{v_l}\frac{1-x}{x}\frac{\rho_v}{\rho_l}\right)^{-1} \quad (15)$$

The ratio v_v/v_l is termed *slip factor* and needs to be given as an experimentally correlated expression [11]. One such correlation for the void fraction for a two-phase water system is given by the Lockart-Martinelli correlation as (16)

$$\alpha = (1 + 0.28X)^{-1} \quad (16)$$

where X is the Martinelli parameter given as in (17)

$$X = 1 + \left(\frac{\rho_v}{\rho_l}\right)^{0.5}\left(\frac{\mu_l}{\mu_v}\right)^{0.5}\left(\frac{1-x}{x}\right)^{0.875} \quad (17)$$

Further, an experimentally determined correlation for the frictional multiplier ϕ is needed. One such correlation, the *Lockart-Martinelli liquid only two-phase frictional multiplier* is given as in (18)

$$\phi_{lo}^2 = \left(1 + \frac{20}{X} + \frac{1}{X^2}\right)(1-x)^{1.75} \quad (18)$$

In this case it implies that there is a *liquid only* velocity defined as $v_{lo} = \frac{\dot{m}_v+\dot{m}_l}{\rho_l(A_v+A_l)}$ and with a *liquid only* Reynolds number given as $Re_{lo} = \rho_l\left(\frac{\dot{m}_v+\dot{m}_l}{\rho_l(A_v+A_l)}\right)d_h/\mu_l = \dot{m}''\, d_h/\mu_l$ where $d_h = 4A/\wp\Delta z$, $\wp$ being the wetted perimeter and $\dot{m}'' = \dot{m}/A$ is the mass flux. These definitions allow the shear stress to be expressed in terms of a *liquid-only shear stress* τ_{lo} and a *two-phase liquid-only frictional multiplier* ϕ_{lo}^2 as $\tau = \tau_{lo}\phi_{lo}^2$ where $\tau_{lo} = C_{flo}\frac{\dot{m}^2}{2\rho_l A^2}$. Assuming a Blasius-type *liquid-only* coefficient of friction (for a smooth tube) as $C_{flo} = 0.079Re_{lo}^{-0.25}$ for turbulent flow and $C_{flo} = 16/Re_{lo}$ for laminar flow, and to ensure non-division, by zero if $Re_{lo} < 1$ as, say $C_{flo} = 16$. Note that taking the Reynolds number as 1181 for the transition from turbulent to laminar flow, and visa verse, ensures that the coefficient of friction C_{flo} is a continuous of Re_{lo} , if deemed appropriate. Maybe one would want to build in some "extra complexity" into the simulation model by introducing some sort of hysteresis, assuming for example, that laminar flow becomes turbulent at *Re* = 2300 and that turbulent flow changes to laminar flow at *Re* = 1800.

3.4 Heat transfer coefficients correlations

Heat transfer coefficients are required to calculate the rate of heat transfer from one medium to another at different temperature. The prediction of the heat coefficients is still a complex matter and to-date there is no comprehensive theory allowing their application in natural convection boiling [12].

There exist many correlations and they are based on the geometry, the type and regime flow that implies for each geometry different correlations for the heat transfer coefficients are required, however most correlations will take the "Nusselt form" [13].

For single phase natural convection free convection is only involved with laminar flow as turbulent is insignificant due to the slow moving fluid near surfaces, thus the Collier correlation as given by (19) is used [14]. In forced flow turbulent convection the Gnielinski correlation heat transfer coefficient given by (22) is used [6].

$$Nu_D = 0.17Re_D^{0.33}Pr^{0.43}\left(\frac{Pr}{Pr_w}\right)^{0.25}Gr^{0.1} \quad Re_D \leq 2000 \tag{19}$$

where Gr is the Grashof number used to assess the impact of natural convection and Pr the Prandtl number are determined using (20) and (21).

$$Gr = \frac{L^3\rho g\beta\Delta T}{\mu^2} \tag{20}$$

where L is the control volume length in the direction of the flow, β is the thermal expansion coefficient and μ is the dynamic viscosity of the fluid.

$$Pr = \frac{c_p\mu_l}{k_l} \tag{21}$$

where c_p is specific heat at constant pressure and k is the thermal conductivity

The Nusselt number of forced convection equation is by (22)

$$Nu_D = \frac{(f/8)(Re_D - 1000)Pr}{1 + 12.7(f/8)^{1/2}(Pr^{2/3} - 1)}; \quad 3000 < Re_D < 10^6 \tag{22}$$

The Rayleigh number Ra correction factor as shown in (23) is introduced [15] when taking in consideration the effects of natural convection in natural circulation.

$$Nu_D = Nu_D Ra^{-0.011} \tag{23}$$

3.5 Numerical simulation model

An explicit numerical solution method is used to solve the set of time dependent temperature coupled partial differential equations (1) to (18) that constitute the theoretical model of the loop. The set of equations are used to simulate the thermo-fluid behaviour of the natural circulation and heat transfer in the loop. Figure 3 shows an applicable i^{th} control volume of the natural circulation loop discretised in series of control volumes as in figure 2, after applying the conservation equations and assumptions stipulated in section 3. The computer program solution algorithm used to solve equations of section 3 is briefly given in appendix A.

4. Results and discussions

Experimental tests for a single to two phase natural circulation loop were conducted in order to validate the thoretical calculated (numerically) thermo-fluid behaviour of the working fluid with a computer algorithm given in appendix A, using Qbasic 64. Results are given in Figure 4 in terms of heat input into the system through the heating plate elements and transient behaviour of the mass flow rate of the working fluid. Table 1 shows the electrical power input, from start-up to shutdown, of a typical single to two phase operating mode. The table shows the percentage of full power, the time at which the power was increased, the equivalent electrical power of each heating section and the total electrical power. The power was increased gradually in steps of 30, 50, 70 and 100 per cent of the full power of 9399.02 W as function of time in order to maintain equilibrium in the loop [9], thus avoiding the transient start-up associated with natural circulation that may be caused if starting the process at a relatively higher power. The power input was shut down at 18000 seconds after the two highes heating elements have reached saturation and the two lowest tended to stabilise and the system was allowed to cool down. To reach the two-phase mode, only on pipe-in-pipe heat exchanger (HE7) was used with a corresponding mass flow rate of 0.09 kg/s.

Table 1. Heating plate electrical power input for experimental test

Power, %	Time, s	Plate 1, W	Plate 2, W	Plate 3, W	Plate 4, W	Total, W
30	0	451.16	451.16	243.04	140.24	1285.60
50	1800	1134.04	1080.00	1080.00	474.79	3768.83
70	5400	2098.29	1984.89	2079.18	960.26	7122.62
100	14404	2734.38	2734.38	2757.20	1173.06	9399.02
0	18000	0.00	0.00	0.00	0.00	0.00

Figure 4(a) shows the power input and power removed as function of time and Figure 4(b) shows temperature profiles of the heating plate elements of the experimental setup as shown in figure 1. The difference observed in these temperature profiles are due to individual resistances and power ratings as depicted in table 1. From figure 4(b) it can be seen that the increase in the input power corresponds with the increase in the heating plates temperatures, however after 11423 seconds when the two top temperatures reached $125.07^{o}C$, no more increase was observed even after 100 per cent of full power was input at t = 144404 s. At the bottom of the heating section of the loop, cold water from the condenser section mixed with hot water, therefore daftecting the two temperature profiles as they show a decrease in temperature of about $15^{o}C$, before they increase again. The lowest heating plate (H1) was more affected by the cold water than the other three heaters and H4 on top was less affected as this can be seen in the circled section of figure 4(b) highlithing the difference in the tempreture profiles.

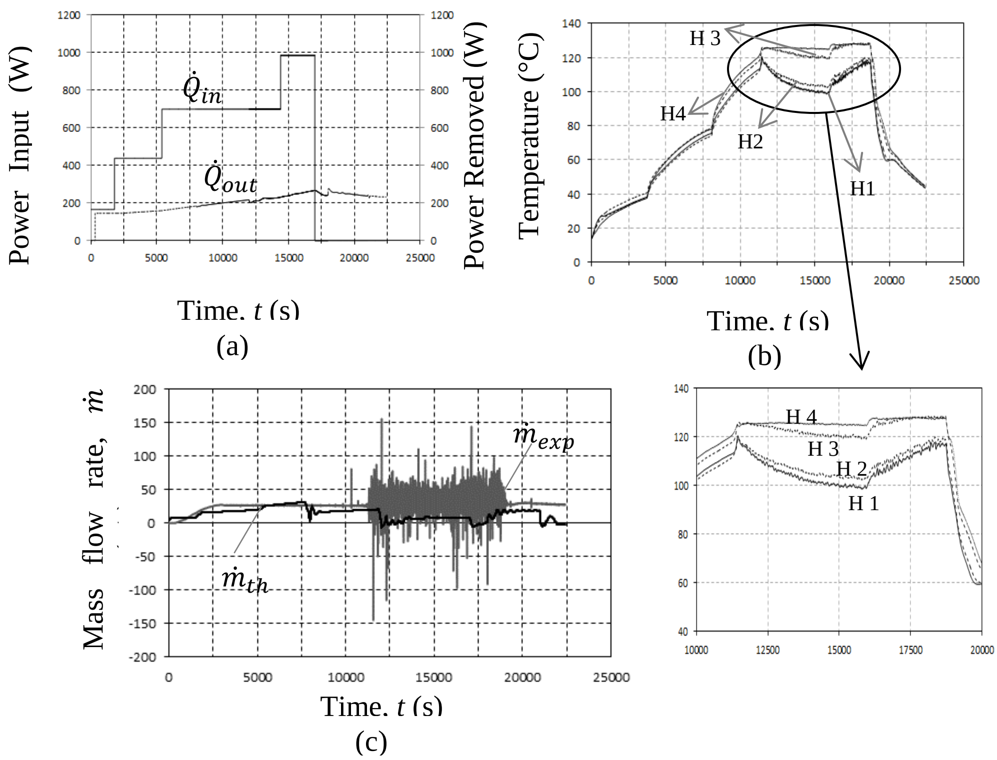

Fig. 4. Experimental and theoretical results; (a) power input vs power output, (b) heating plates temperatures and (c) mass flow rates as a function of time

Figure 4(c) shows the experimental and theoretical mass flowrate behaviour of the working fluid. The experimental mass flow rate is as measured by the pressure drop over the orifice plate (see figure 1). At *t* = 1800 the power was increased to 50 per cent of full power. At this point only the single phase is observed and the mass flow rate increased steadly to tabilise at about 20 kg/s after 5000 seconds of experimental test. With more heat added to the system small bubbles started to appear and when the power was increased to 70 per cent of full power, the number of bubbles also increased giving way to the two-phase flow in the loop. After 2010 s with 70 percent of full power (9.399 kW) boiling occured and this can be in the mass flow rate profile behaviour showing a more dynamic oscillatory behaviour. This behaviour brings both accoustic and density waves in the loop, a typical characteristic of the transient two-phase flow instabilities [16].

Theoretical results are more or less in line with the experimental results, however the experimental show more oscillatory behaviour (instabilities) due to the sensibilities of the measuring instruments and the working conditions, while the theoretical are done in a more stable condition, but with the same power input and time step as the experimental. Both profiles showed that boiling occured at about the same time and have similar single phase and two phase behaviours, therefore adding confidence in the validity of the results using the Martenilli two-phase flow correlations detailled in section 3.

At *t* = 18000 s, power was switched off and both the heating plates and the working fluid were allowed to cool down for about 2500 s before the test was stopped. In order to achieve the two-phase flow and consequently boiling, only one heat exchanger (the one located in the top of the condenser section or HE7) was used while the other six were bypassed.

5. Conclusion and recommendations

Information collected through the literature review shows that the basic approach in theoretically simulating the single and two-phase flow using the separated model is to discretize the loop into a series of parallel one-dimensional axially symmetrical control volumes, in which the two-phases are treated as two separate fluids [10]. The loop was thus discretised and conservation equations of mass, momentum and energy were applied. Theoretical results were then generated through numerical solution for the single to two-phase operating mode of the loop. This shows that transient behaviours of the flow were successfully investigated as the results shown in Figure 4(c) correlate well the theoretical to the experimental findings.

In conclusion, the theoretical calculated thermo-fluid parameters of the natural circulation loop of this paper using the separated two-phase model adequately represented the actual transient and dynamic flow and heat transfer behaviour of the loop, thereby validating the results with the experimental values although there are areas that require improvements. This model can therefore be confidently used in future two-phase flow studies.

Appendix A

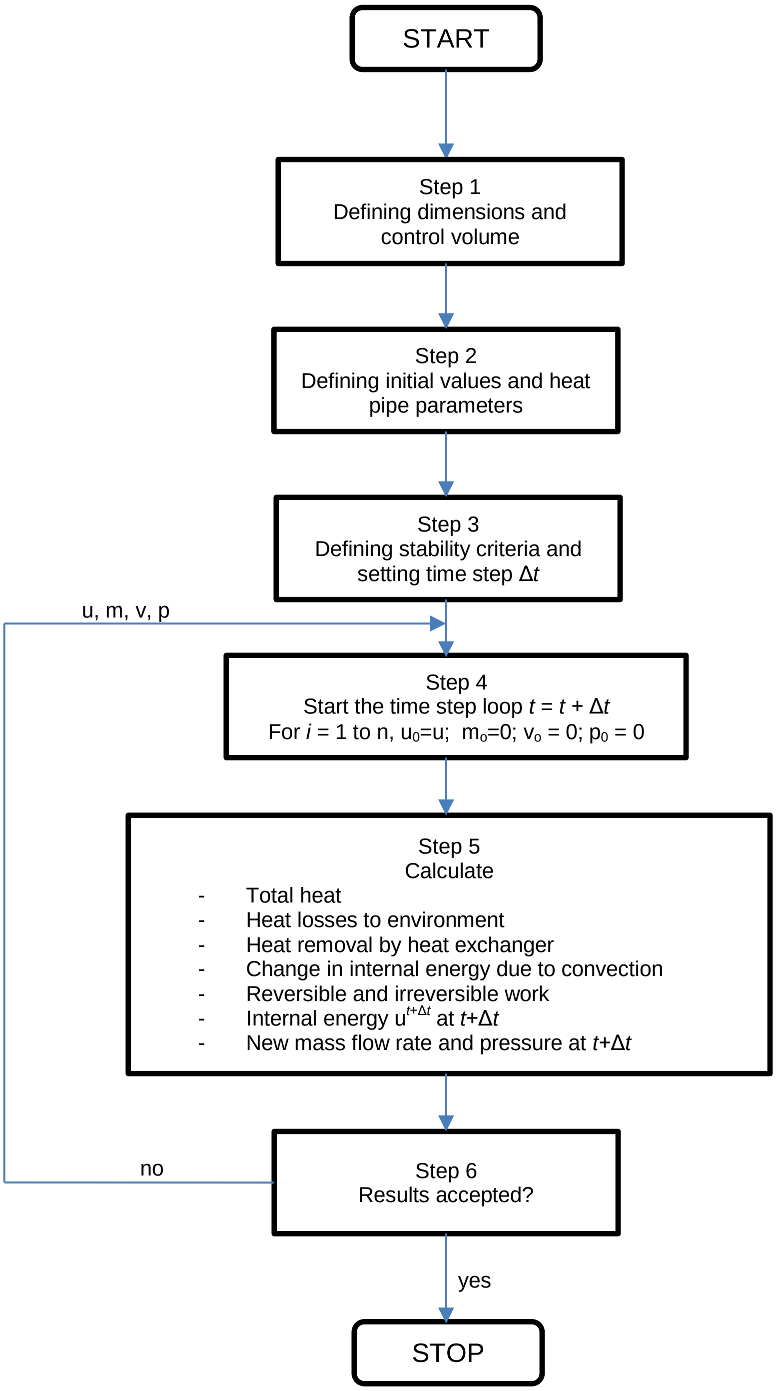

Fig. A.1. Numerical solution computer program algorithm

Nomenclature

a acceleration, m/s^2

A area, m^2

A_x cross sectional area, m^2

A_z heat transfer area, m^2

c specific heat, (c_p, c_v) J/kgK

C_f coefficient of friction
d diameter, m
f Darcy friction factor, two-phase flow friction factor
g Gravity, saturated gas
G force due to gravity, N; mass flux, kg/s/m^2
G Grashof number $Ga = \frac{g\beta(T_W - T)d^3}{v^2}$
k Thermal conductivity
l length, m
L length, m
m mass, kg
$\dot{m}$ mass flow rate, kg/s
N Number
Nu Nusselt number, $Nu = hd/k$
P pressure, Pa
Pr Prandtl number, $Pr = \mu c_p/k$
$\dot{Q}$ heat flow rate, W
Re Reynolds' number $Re = \rho v d/\mu$
S slip factor; Suppression factor
T temperature, K, °C; period, s
t time, s
u specific internal energy, J/kg
v velocity, m/s
V volume, m^3
x mass fraction ; thermodynamic quality; displacement, m
X Martinelli parameter
z distance, m

Greek symbols
α void fraction
β thermal expansion coefficient, K^{-1}
θ inclination angle, rad
μ dynamic viscosity, Ns/m^2
ρ density, kg/m^3
$\wp$ perimeter, m
τ shear stress, N/m^2
ϕ^2 two-phase frictional multiplier

Superscript
t time
Δt time step

Subscripts

atm atmospheric

D diameter

f saturated liquid; friction

g gas

G gravity

h hydraulic; wetted perimeter; homogeneous

i i^{th} control volume or element

in inlet

l liquid

L length

lo liquid only

loss loss

M momentum

minor minor losses

o only; outside

out outlet

q constant heat flux

r reference

sat saturated

T constant temperature

Tot total

v vapour

w water, wall

x at a particular point along the surface

Abbreviations

BL Bottom Left

BR Bottom Right

CV Control Volume

H Heater, Heating element

HE Heat Exchanger

LHS Left Hand Side

NC Natural Circulation

P Pressure

RCCS Reactor Cavity Cooling System

RHS Right Hand Side

TL Top Left

TR Top Right

References

[1] Ruppersberg J. & Dobson R., 2007. Flow and heat transfer in a closed loop thermosyphon Part II - experimental simulation. Journal of Energy in Southern Africa, Volume 3, pp. 41 - 48.

[2] Grief R., 1988. Natural circulation loops. ASME J. Heat Transfer, Volume 110, pp. 1243-1258.

[3] Bieliński, H. & Mikielewicz, J., 2011. Natural circulation in single and two phase thermosyphon loop with conventional tubes and minichannels. The Szewalski Institute of Fluid-Flow Machinery, Volume 14, pp. 475-494.

[4] Sittmann I., 2010. Inside-pipe heat transfer coefficient characterisation of a one third height scale model of a natural loop suitable for reactor cavity cooling system of the PMBR, Stellenbosch: MSc Thesis, Stellenbosch University

[5] Shih Y., 2009. Basic equation in integral form for a control volume. Fluid mechanics, Spring.

[6] Mills, A. & Ganesan, V., 2015. Forced-convection boiling and condensation; Pressure drop. In: Heat Transfer. Delhi, India: Pearson Education, pp. 616-632.

[7] White, F. (2006). Viscous Fluid Flow 3rd Edition. McGraw-Hill.

[8] Cengel, Y. and Boles, M., 2014. Thermodynamics, An Engineering Approach 7th Edition. New York: McGraw Hill.

[9] Whalley, P., 1987. Boiling, condensation and gas-liquid flow, Oxford: Clarendon Press.

[10] Carey, V., 1992. Liquid-vapor phase-Change phenomena, s.l.: Hemisphere.

[11] Chisholm, D., 1983. Two-Phase Flow in Pipelines and Heat Exchangers. New York, Longman Inc.

[12] Beck, J., Blackwell, B. & Clair, C. R. S., 1985. Inverse Heat Conduction. Ill-posed Problems. New York, John Wiley & Sons.

[13] Brodkey, R.S. and H.C. Hershey, Transport Phenomena: A Unified Approach, McGraw-Hill, 1988, pp. 510-15.

[14] Collier, J. & Thome, J., 1996. Basics equations of two-phase models. In: O. E. S. Series, ed. Convective boiling and condensation. Oxford: Claredon Press, pp. 39-56; 67-70.

[15] Yang, R., Liu, R., Zhong, Y. & Liu, T., 2006. Experimental study on convective heat transfer of water flow in a heated tube under natural circulation. Nuclear Engineering and Design, Volume 236, pp. 1902 - 1908.

[16] Vijayan, P. & Nayak, A., 2010. Introduction to instabilities in natural circulation systems, Trieste: In: IAEA Training Course on Natural Circulation Phenomena and Passive Safety Systems in Advanced Water-cooled Reactors, ICTP.